J|A|C|S
ARTICLES
Published on Web 04/20/2005

Dynamic and Structural NMR Studies of Cavitand-Based Coordination Cages

Daniele Zuccaccia,[†] Laura Pirondini,[‡] Roberta Pinalli,[‡] Enrico Dalcanale,*[,‡] and Alceo Macchioni*[,†]

Contribution from the Dipartimento di Chimica, Università di Perugia, Via Elce di Sotto, 8-06123 Perugia, Italy, and Dipartimento di Chimica Organica e Industriale ed Unità INSTM, Università di Parma, Parco Area delle Scienze, 17/A-43100 Parma, Italy

Received December 23, 2004; E-mail: alceo@unipg.it; enrico.dalcanale@unipr.it

Abstract: The interionic structure, kinetic stability, and degree of anion encapsulation of coordination cages **1** were studied by PGSE, NOE, and EXSY NMR techniques. The rate constants for the formation/dissociation processes at 296 K were obtained independently via ^{1}H-NOESY and ^{19}F-NOESY experiments giving, respectively, $k_{obs} = 0.30 \pm 0.04$ s^{-1} in $CDCl_3$ and $k_{obs} = 5.2 \pm 0.8$ s^{-1} in CD_3NO_2/CDC_{13} (7.1) mixture with the proton probe, and $k_{obs} = 0.33 \pm 0.06$ s^{-1} in $CDCl_3$ and $k_{obs} = 5.0 \pm 0.8$ s^{-1} in CD_3NO_2/CDC_{13} (7/1 mixture) with the ^{19}F probe. PGSE experiments showed that in $CDCl_3$ not only the encapsuled anion but also the external anions translate with the same rate as the cage. ^{19}F,^{1}H-HOESY experiments indicated that an average of five external triflate anions are located in the equatorial sites close to the palladium moieties, while two of them approach the polar pockets formed by the alkyl chains. In a $CD_3NO_2/CDCl_3$ (7/1) mixture only one or two anions are in close proximity with the cage, while the others are solvated. In all the considered solvents (benzene, chloroform, methylene chloride, and nitromethane) the inclusion of a single unsolvated triflate anion in the cage is quantitative. ^{19}F,^{1}H-HOESY experiments indicated that the charged guest head points toward one metal center. Therefore, while the ionic aggregation level and kinetic stability of coordination cages **1** are solvent dependent, anion encapsulation is not.

Introduction

Self-assembly has proven to be an extremely effective approach to the generation of molecular capsules[1] and coordination cages.[2] Compared to covalently linked carcerands,[3] both H-bonded capsules and coordination cages are not indefinitely stable.[4] The kinetic lability of the noncovalent connections among the constituent units of these supramolecular species is necessary for allowing the thermodynamic control of the self-assembly processes, which brings in highly desired features such as reversibility, selection, and self-repairing properties.[5] Therefore, understanding the solution dynamics exhibited by these supramolecular assemblies is essential to control their formation and properties.[6] For example, measuring the formation/dissociation kinetics of coordination cages is pivotal for exploiting their inclusion properties in solution and for controlling their assembly on surfaces.[7] In this context, very few studies have been conducted on the kinetic stability of H-bonded capsules,[8] and none on coordination cages, even if suitable spectroscopic techniques are available.[9]

Two other pieces of information are crucial for the characterization of noncovalent supramolecular architectures in solution: the relative positioning of the constituting units and the size of the adducts. This essential information can be obtained by exploiting NOE (nuclear Overhauser effect)[10] and PGSE (pulsed field gradient spin−echo)[11] NMR techniques, respectively. Such techniques have been successfully used for the determination of the interionic structure of intermolecular

[†]Università di Perugia.
[‡]Università di Parma.

(1) (a) Conn, M. M.; Rebek, J., Jr. *Chem. Rev.* **1997**, *97*, 1647−1668. (b) MacGillivray, L. R.; Atwood, J. L. *Angew. Chem., Int. Ed.* **1999**, *38*, 1018−1033. (c) Hof, F.; Craig, S. L.; Nuckolls, C.; Rebek, J., Jr. *Angew. Chem., Int. Ed.* **2002**, *41*, 1488−1508. (d) Corbellini, F.; Fiammengo, R.; Timmerman, P.; Crego-Calamata, M.; Versluis, K.; Heck, A. J. R.; Luyten, I.; Reinhoudt, D. N. *J. Am. Chem. Soc.* **2002**, *124*, 6569−6575.
(2) (a) Fujita, M.; Umemoto, K.; Yoshizawa, M.; Fujita, N.; Kusukawa, T.; Biradha, K. *Chem. Commun.* **2001**, 509−518. (b) Caulder, D. L.; Raymond, K. N. *Acc. Chem. Res.* **1999**, *32*, 975−982. (c) Seidel, S. R.; Stang, P. J. *Acc. Chem. Res.* **2002**, *35*, 972−983.
(3) Cram, D. J.; Cram, J. M. In *Container Molecules and their Guests, Monographs in Supramolecular Chemistry*; Stoddart, J. F., Ed.; Royal Society of Chemistry: Cambridge, 1994; Vol. 4.
(4) Sherman, J. C. *Tetrahedron* **1995**, *51*, 3395−3422.
(5) Lindsey, J. S. *New J. Chem.* **1991**, *15*, 153−180.
(6) Davis, A. V.; Yeh, R. M.; Raymond, K. N. *Proc. Natl. Acad. Sci. U.S.A.* **2002**, *99*, 4793−4796.
(7) (a) Levi, S.; Guatteri, P.; van Veggel, F. C. J. M.; Vancso, G. J.; Dalcanale, E.; Reinhoudt, D. N. *Angew. Chem., Int. Ed.* **2001**, *40*, 1892−1896. (b) Menozzi, E.; Pinalli, R.; Speets, E. A.; Ravoo, B. J.; Dalcanale, E.; Reinhoudt, D. N. *Chem. Eur. J.* **2004**, *10*, 2199−2206.
(8) (a) Mogck, O.; Pons, M.; Böhmer, V.; Vogt, W. *J. Am. Chem. Soc.* **1997**, *119*, 5706−5712. (b) Szabo, T.; Hilmersson; Rebek, J., Jr. *J. Am. Chem. Soc.* **1998**, *120*, 6193−6194. (c) Vysotsky, M. O.; Thondorf, I.; Böhmer, V. *Angew. Chem., Int. Ed.* **2000**, *39*, 1264−1267.
(9) For a review on dynamic NMR studies of supramolecular complexes see: Pons, M.; Millet, O. *Prog. Nucl. Magn. Reson. Spectrosc.* **2001**, *38*, 267−324.
(10) Neuhaus, D.; Williamson, M. *The Nuclear Overhauser Effect in Structural and Conformational Analysis*; Wiley-VCH: New York, 2000.
(11) (a) Johnson, C. S., Jr. *Prog. Nucl. Magn. Reson. Spectrosc.* **1999**, *34*, 203−256. (b) Price, W. S. *Concepts Magn. Reson.* **1997**, *9*, 299−336. (c) Price, W. S. *Prog. Nucl. Magn. Reson. Spectrosc.* **1998**, *10*, 197−237. (d) Stilbs, P. *Prog. Nucl. Magn. Reson. Spectrosc.* **1987**, *19*, 1−45. (e) Stejskal, E. O.; Tanner, J. E. *J. Chem Phys.* **1965**, *42*, 288−292.

metallorganic adducts in solution[12,13] and labile supramolecular assemblies.[14−16]

In this paper, we report the results of the application of PGSE and NOE NMR methodologies to the investigation of cavitand-based coordination cages.[17] Among the different coordination cages available in our group, we chose nitrile-based cages of general structure **1**[18] for this study, because of their anion inclusion properties.[19] Two major features of coordination cages **1** turned out to be appealing: (i) the included counterion can be easily distinguished from the external ones via ^{19}F NMR; (ii) the anion exchange with the bulk requires the dissociation of the cage, since the lateral portals of **1** are too small to allow guest permeation. These features define the included anion as a unique probe to assess the kinetic stability of this class of coordination cages. In detail, the interionic structure of the coordination cages in solution, i.e., their hydrodynamic radius, their tendency to aggregate, the positioning of the external anions with respect to the multicationic cage, and the orientation of the encapsulated anion, has been studied through PGSE and ^{19}F,^{1}H-HOESY (heteronuclear Overhauser effect spectroscopy) NMR techniques, while EXSY NMR (exchange spectroscopy) experiments[20] have been used to investigate their kinetic stability.

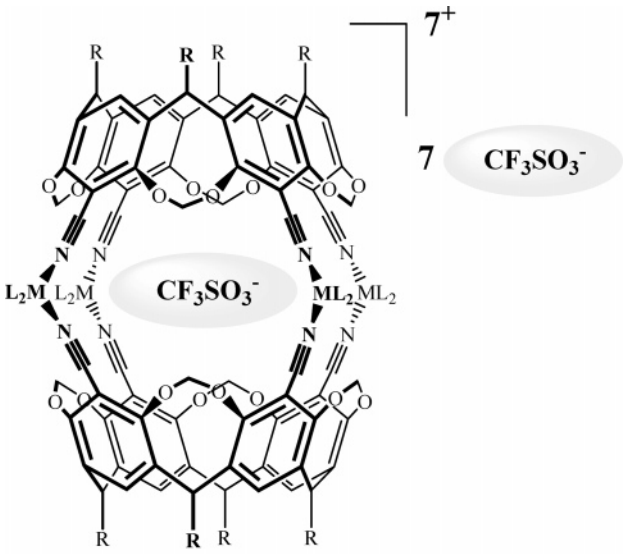

Structure 1

Results and Discussion

Empty versus Occupied Cages. The equilibrium reaction between cavitand **2a** and palladium complex **3a** that leads to the self-assembly of the coordination cage **1a** (Scheme 1, dppp = 1,2-bis(diphenylphosphino)propane) was investigated in benzene-d_6, chloroform-*d*, methylene chloride-d_2, and nitromethane-d_3 by means of quantitative integration of ^{1}H, ^{31}P, and ^{19}F NMR spectra.

It is known that complex **3a** in wet solvents reacts with water, forming a small amount of the bis-aquo complex [Pd(dppp)-$(H_2O)_2$]$(CF_3SO_3)_2$ (**4**).[21] The ^{31}P NMR spectra clearly indicated that, when solutions of cavitand **2a** and complex **3a** were mixed together in a 2/4 stoichiometry, complex **3a** quantitatively reacted, while a variable amount of **4** remained in solution, together with the corresponding uncomplexed cavitand. The relative amounts of **4** and of the formed cage **1a** were determined by integrating their resonances in the ^{31}P NMR spectra. To determine the percentages of coordination cages having an encapsulated counterion ($CF_3SO_3^-{}_{in}$), its ^{19}F NMR resonance and that of the external ($CF_3SO_3^-{}_{out}$) counterions were integrated. It is important to stress that the ^{19}F resonance relative to $CF_3SO_3^-{}_{out}$ is due not only to the cage **1a** but also to the water complex **4**. Once the contribution of complex **4** to $CF_3SO_3^-{}_{out}$ has been subtracted taking into account the ^{31}P NMR spectra, the molar ratio $CF_3SO_3^-{}_{out}/CF_3SO_3^-{}_{in}$ of cage **1a** and, consequently, the relative amount of cages bearing an encapsulated counterion and the empty ones were obtained. The results are reported in Table 1.

The percentage of coordination cage **1a** bearing $CF_3SO_3^-{}_{in}$ is higher than 95%, and, considering that such values derive from a process of double integration, the a priori maximum error is comparable with the amount of empty cages (<5%). Consequently, it is reasonable to regard the encapsulation process as quantitative. This result is supported by the crystal structure of **1c**, where every cage contains a single unsolvated triflate anion.[19]

Interionic Structure. The tendency to form aggregates and the relative anion-cage position were investigated in solution by means of PGSE and NOE NMR experiments, respectively. ^{19}F and ^{1}H PGSE NMR measurements help determine the translational self-diffusion coefficient (D_t) of the anion and the coordination cage, respectively. D_t is related to the hydrodynamic radius (r_H) of the diffusing particle according to a modified Stokes−Einstein equation: $D_t = kT/c\pi\eta r_H$ (where k is the Boltzman constant, T is the temperature, c is a numerical factor that can be expressed as a function of r_H and the van der Waals radius of the solvent,[22] and η is the solution viscosity). The diffusion coefficient D_t can be estimated with different methodologies: (1) by measuring the proportionality constant using a sample of HDO (5%) in D_2O in the same exact conditions of the sample of interest; (2) by calibrating accurately the gradient used in the sequence. In both cases the results can be precise but not accurate, due to the presence of different sources of possible errors. In particular, the inaccuracy can derive from (i) convection currents (mass convection) when solvents with low viscosity are used, (ii) changes in solution

(12) (a) Macchioni, A. *Eur. J. Inorg. Chem.* **2003**, 195−205, and references therein. (b) Binotti, B.; Macchioni, A.; Zuccaccia, C.; Zuccaccia, D. *Comments Inorg. Chem.* **2002**, *23*, 417−450. (c) Macchioni, A. In *Perspectives in Organometallic Chemistry*; Screttas, C. G., Steele B. R., Eds.; The Royal Society of Chemistry: Cambridge, 2003; pp 196−207.
(13) Pregosin, P. S.; Martinez-Viviente, E.; Kumar, P. G. A. *Dalton Trans.* **2003**, 4007−4014.
(14) Cohen, Y.; Avram, L.; Frish, L. *Angew. Chem., Int. Ed.* **2005**, *44*, 520−554, and references therein.
(15) For PGSE studies on coordination cages and squares see: (a) Olenyuk, B.; Levin, M. D.; Whiteford, J. A.; Shield, J. E.; Stang, P. J. *J. Am. Chem. Soc.* **1999**, *121*, 10434−10435. (b) Otto, W. H.; Keefe, M. H.; Slan, K. E.; Hupp, J. T.; Larive, C. K. *Inorg. Chem.* **2002**, *41*, 6172−6174.
(16) For NOE studies on coordination cages see: (a) Bourgeois, J.-P.; Fujita, M.; Kawano, M.; Sakamoto, S.; Yamaguchi, K. *J. Am. Chem. Soc.* **2003**, *125*, 9260−9261. (b) Kumazawa, K.; Yamanoi, Y.; Yoshizawa, M.; Kusukawa, T.; Fujita, M. *Angew. Chem., Int. Ed.* **2004**, *43*, 5936−5940.
(17) Pirondini, L.; Dalcanale, E. *Encyclopedia of Nanoscience and Nanotechnology*; Marcel Dekker: New York, 2004; pp 3415−3430.
(18) Jacopozzi, P.; Dalcanale, E. *Angew. Chem., Int. Ed. Engl.* **1997**, *36*, 613−615.
(19) Fochi, F.; Jacopozzi, P.; Wegelius, E.; Rissanen, K.; Cozzini, P.; Marastoni, E.; Fisicaro, E.; Manini, P.; Fokkens, R.; Dalcanale, E. *J. Am. Chem. Soc.* **2001**, *123*, 7539−7552.
(20) Perrin, C. L.; Dwyer, T. J. *Chem. Rev.* **1990**, *90*, 935−967.
(21) Gorla, F.; Venanzi, L. M. *Helv. Chim. Acta* **1990**, *73*, 690−697.
(22) (a) Gierer, A.; Wirtz, K. *Z. Naturforsch. A* **1953**, *8*, 522−532. (b) Spernol, A.; Wirtz, K. *Z. Naturforsch. A* **1953**, *8*, 532−538. (c) Espinosa, P. J.; Garcia de la Torre, J. *J. Phys. Chem.* **1987**, *91*, 3612−3616. (d) Chen, H.-C.; Chen, S.-H. *J. Phys. Chem.* **1984**, *88*, 5118−5121.

Scheme 1. Self-Assembly of Coordination Cages **1a**−**c**

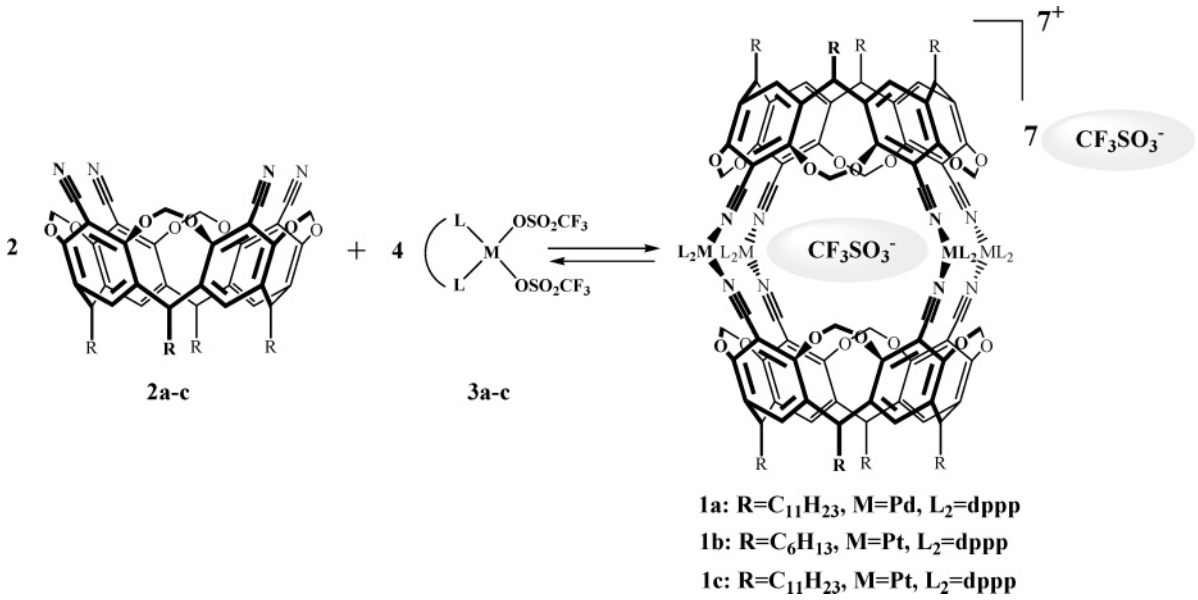

Table 1. Experimental $[CF_3SO_3^-{}_{out}]/[CF_3SO_3^-{}_{in}]$ Ratios for Coordination Cage **1a** and the Derived Molar Percentages of Cages with Encapsulated Anion in Various Solvents at 298 K

	$[CF_3SO_3^-{}_{out}]/[CF_3SO_3^-{}_{in}]$ of **1a**	cages **1a** with encaps. anion (%)
benzene-d_6	7.4	95
chloroform-*d*	7.1	99
methylene chloride-d_2	7.3	96
nitromethane-d_3	7.4	95

viscosity when the dependence of the diffusion coefficients (and so the aggregation size) on the concentration needs to be known. In addition, the absolute temperature and the viscosity of the solution must be evaluated accurately to obtain a consistent value of hydrodynamic radius (r_H). A methodology that allows the determination of r_H in a simple and more accurate way consists of the use of an internal standard;[12b,12c,23] this approach circumvents the dependence of the D_t values on temperature, solution viscosity, and gradient calibration (for details see the Experimental Section).

From the experimentally determined D_t values, r_H (and *c* factors) of the species present in solution were estimated. Representative ^{19}F and ^1H PGSE NMR experiments are illustrated in Figures 1 and 2, respectively, using tetrakis(trimethylsilyl)silane (TMSS) as internal standard in the case of ^1H PGSE. Data are reported in Table 2. The resonance attributions of both cavitand **2a** and cage **1a** are reported in the Experimental Section.

As a general comment, the hydrodynamic radii obtained in solution (12.9−13.7 Å) cannot be directly compared with those in the solid state because of the innumerable conformational degrees of freedom of the long hydrocarbon chains ($C_{11}H_{23}$). The distances from the center of the cage **1a** and the external phosphine protons and the chain protons, almost completely elongated, are 12.7 Å and ca. 16 Å, respectively, in reasonably good agreement with the values found in solution. By comparing the diffusion coefficients of cage **1a** with those of the triflate anions, it can be seen that the encapsulated anion $CF_3SO_3^-{}_{in}$ translates exactly with the same velocity as the cage in all the solutions (entries 2−4 in Table 2), and consequently, its apparent hydrodynamic radius is the same as those of the cage. As stated in the previous section, all the coordination cages **1** bear an encapsulated anion. Interestingly, the external anion $CF_3SO_3^-{}_{out}$ in chloroform has self-diffusion coefficients much higher than that expected based on its van der Waals radius (2.6 Å) and, in the case of the most concentrated solution (entry 3, 6 mM), approaches that of **1a**. In the ^{19}F NMR spectra we should observe two resonances due to $CF_3SO_3^-{}_{out}$ and $CF_3SO_3^-{}_{in}$ with an intensity ratio 7/1, but in reality higher values were obtained: 10/1 for entry 2 (**1a** 1.5 mM), 8/1 for entry 3 (**1a** 6.0 mM), and 25/1 for entry 4 (**1a** 0.4 mM). The higher intensity of the resonance attributed to $CF_3SO_3^-{}_{out}$ is due to complex **4**, as discussed in the previous section. After having extracted from the D_t values of $CF_3SO_3^-{}_{out}$ the contribution of those anion that belong to complex **4**, whose radius was estimated to be ca. 5

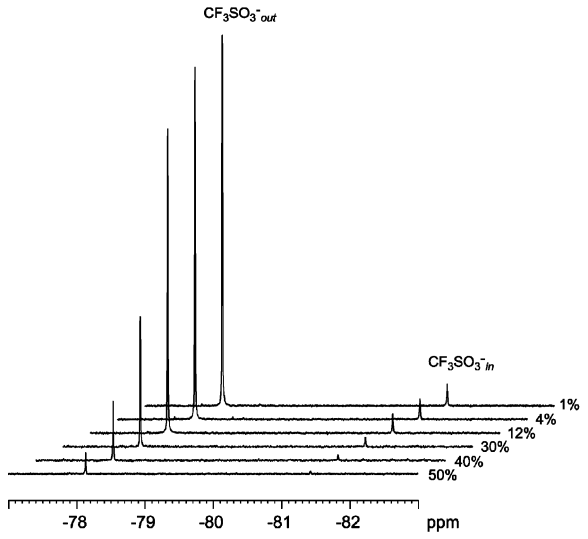

Figure 1. ^{19}F PGSE NMR spectra recorded in chloroform-*d* showing the dependence of the resonance intensities on the intensity of the pulsed-field gradient.

(23) Babushkin, D. E.; Brintzinger, H. H. *J. Am. Chem. Soc.* **2002**, *124*, 12869−12863.

Table 2. Diffusion Coefficients ($10^{10}D_t$ m^2 s^{-1}) and Hydrodynamic Radii (r_H, Å) for **1a**, **2a**, $CF_3SO_3^-{}_{in}$, and $CF_3SO_3^-{}_{out}$ in Chloroform-*d* (entry 1: [**2a**] = 6 mM; entry 2: [**1a**] = 1.5 mM and [**2a**] = 6 mM; entry 3: [**1a**] = 6 mM and [**2a**] = 24 mM) and in Nitromethane-d_3/Chloroform-*d* (7/1) (entry 4: [**1a**] = 0.4 mM and [**2a**] = 3 mM)

entry	D_t(**1a**)	D_t(**2a**)	$D_t(CF_3SO_3^-{}_{in})$	$D_t(CF_3SO_3^-{}_{out})$	r_H(**1a**)	r_H(**2a**)	$r_H(CF_3SO_3^-{}_{in})$	$r_H(CF_3SO_3^-{}_{out})$
1		5.3				8.0		
2	3.1	5.0	3.1	4.0	12.9	8.1	12.9	10.1
3	2.7	4.2	2.7	2.9	13.7	9.0	13.5	13.0
4	2.5	3.9	2.5	8.7	13.0	8.5	13.0	4.3

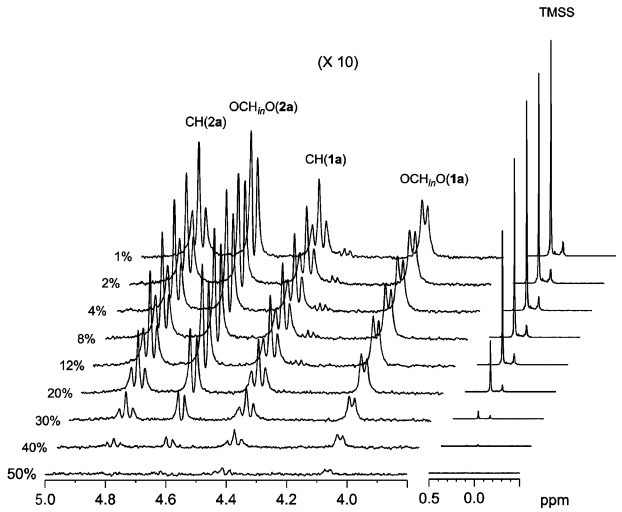

Figure 2. Two sections of the ^{1}H PGSE NMR spectra recorded in chloroform-*d* showing the dependence of the resonance intensities, resorcinarene CH and inward hydrogen of the methylene bridges ($OCH_{in}O$), on the intensity of the pulsed-field gradient.

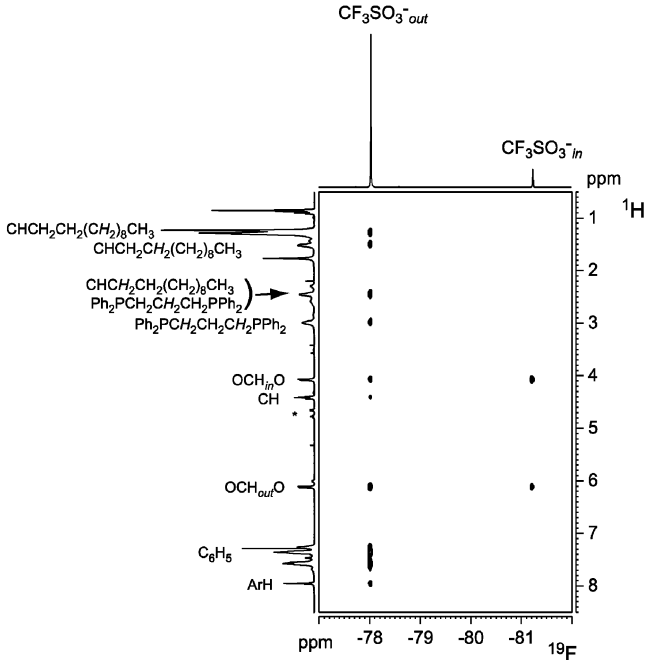

Figure 3. ^{19}F,^{1}H-HOESY NMR spectrum (376.65 MHz, 296 K, chloroform-*d*) of coordination cage **1a**. *Denotes resonances of cavitand **2a**.

Table 3. Relative NOE Intensities Determined for a Solution 6.0 × 10^{-3} M in Chloroform-*d* of **1a** by Arbitrary Fixing at 1 the Intensity of the NOE(s) between the Anion Resonances and the Aryl Protons of dppp for $CF_3SO_3^-{}_{out}$ and the Anion Resonances and $OCH_{in}O$ for $CF_3SO_3^-{}_{in}$

	$CF_3SO_3^-{}_{in}$	$CF_3SO_3^-{}_{out}$
Ar*H*		0.24
o-C_6H_5		0.94
m,*p*-C_6H_5		1.00
$OCH_{out}O$	0.57	0.60
CH		0.11
$OCH_{in}O$	1.00	0.26
$Ph_2PCH_2CH_2CH_2PPh_2$		0.20
$CHCH_2(CH_2)_9CH_3$ $Ph_2PCH_2CH_2CH_2CH_2PPh_2$		0.30
$CHCH_2CH_2(CH_2)_8CH_3$		0.22
$CHCH_2CH_2(CH_2)_8CH_3$		0.14

Å, an apparent r_H very close to that of cage **1a** is obtained for entries 2 and 3. This means that all seven external anions are aggregated with the cationic cage in chloroform-*d*. By applying the same procedure to the mixture nitromethane-d_3/chloroform-*d* (7/1) (entry 4), where $CF_3SO_3^-{}_{out}$ has a self-diffusion coefficient much larger than that of **1a**, it can be deduced that only ca. 15% of the anions translate with cage **1a**. This means that only an average of one or two anions of the seven $CF_3SO_3^-{}_{out}$ remain aggregated to the multicationic coordination cage **1a** in this highly polar solvent mixture.

^{19}F,^{1}H-HOESY NMR experiments help determine the anion−cation relative position since the observed heteronuclear NOEs have an intensity that is proportional to the inverse of the sixth power of the internuclear distance.[10] From a qualitative point of view, if an NOE is observed, then the two interacting nuclei are closer in space than 5 Å. On the other hand, a quantitative comparison between two different NOEs requires that a mixing time in the initial linear buildup of the NOE is used and that the recycle delay is higher than 5 times the longitudinal relaxation time (T_1).[10] After having evaluated T_1 for both protons and fluorine atoms (data are reported in the Experimental Section), quantitative ^{19}F,^{1}H-HOESY NMR spectra were recorded in chloroform-*d* (Figure 3), where PGSE results indicate the presence of adducts in which all seven $CF_3SO_3^-{}_{out}$ translate with the multicationic cage. The NOE volumes, scaled for the number of equivalent nuclei according to the Ernst−Macura equation,[24] are reported in Table 3.

From both Figure 3 and Table 3 it can be seen that $CF_3SO_3^-{}_{in}$ selectively interacts with the OCH_2O protons. The interaction intensity is higher with the proton that points inside the cage ($OCH_{in}O$) than with the one that points outside ($OCH_{out}O$). It appears that $CF_3SO_3^-{}_{in}$ orients its "negative head" toward the 2-fold positively charged Pd atoms and the "CF_3-tail" toward the OCH_2O moiety. The $CF_3SO_3^-{}_{out}$ anions weakly interact with protons belonging to the R groups of cavitand **1a** at the lower rim, in particular with the first two methylene and methyne groups. Further weak interactions are present with the aromatic protons at the bottom of the resorcinarene skeleton. The preference of anions such as bromide and chloride for the pocket formed by the four pendant alkyl groups has been observed in the solid state in the case of hydrogen-bonded resorcinarene capsules, and it has been attributed to weak CH···X^- interac-

(24) Macura, S.; Ernst, R. R. *Mol. Phys.* **1980**, *41*, 95−117.

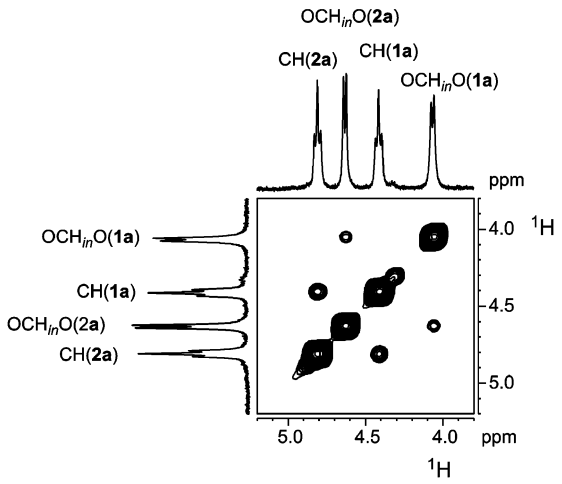

Figure 4. Section of the ^{1}H-NOESY NMR spectrum (400.13 MHz, 296 K, chloroform-*d*, $\tau_m = 400$ ms) pertinent to an equilibrium mixture between **1a** and **2a**.

tions.[25] The fact that the same preference is retained in solution in the case of triflate is intriguing, suggesting that multiple CH···X$^-$ interactions successfully compete with anion solvation in chloroform, with the help of some residual electrostatic interaction. The strongest contacts for $CF_3SO_3^-{}_{out}$ are (1) with the aryl protons of dppp and (2) with the methylene protons $OCH_{in}O$ and $OCH_{out}O$. These results suggest that the $CF_3SO_3^-{}_{out}$ anions are prevalently positioned on the "equatorial" plane containing the four palladium(II) atoms, and in particular external anions are close to the dppp ligand. A recent crystal structure of a nanoscale coordination cage revealed that, when the space in the equatorial region is sufficient, all triflates are positioned outside the cavity, near the four metal centers.[26] This should be the preferred location for the anions in order to maximize electrostatic interactions with the metal cations. The inability to place all seven $CF_3SO_3^-{}_{out}$ close to the metal centers in **1** for steric reasons makes the hydrocarbon pockets in the polar regions an alternative site for at least two triflates.

Kinetic Stability of Coordination Cages. Exchange cross-peaks between ^{1}H resonances of coordination cage **1a** and those of cavitand **2a** and between $CF_3SO_3^-{}_{in}$ and $CF_3SO_3^-{}_{out}$ were observed in ^{1}H-NOESY and ^{19}F-NOESY NMR spectra, respectively. Quantitative ^{1}H-NOESY and ^{19}F-NOESY NMR experiments were carried out with a mixing time ranging from 0.1 to 1.2 s for cage **1a** and cavitand **2a** in chloroform-*d* and nitromethane-d_3/chloroform-*d* (7/1) at different molar fraction values. In Figures 4 and 5, ^{1}H-NOESY and ^{19}F-NOESY NMR spectra for **1a** and **2a** in chloroform-*d*, respectively, are shown. Plots of the experimental values of $\ln[(r-1)/(r+1)]$ (where r depends on both the molar fraction of the species that undergo the dynamic process and the volume of diagonal and cross-peaks, as described in the Experimental Section) versus the mixing time τ_m are reported in Figures 6 and 7. The slopes of the linear part of the plots at short mixing time values (from 0 to 400 ms) afforded the observed rate constants (k_{obs}). In the ^{1}H-NOESY spectra, the exchange peaks of the CH resonances (resorcinarene bridging methynes) were investigated due to their

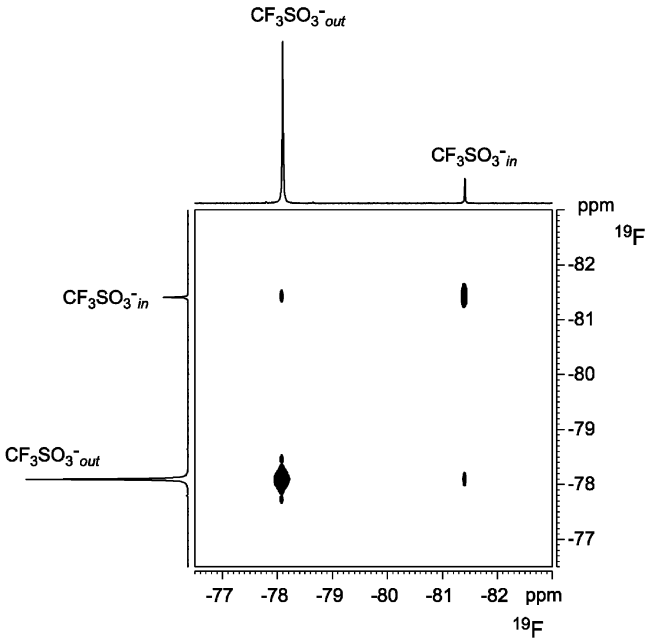

Figure 5. ^{19}F-NOESY NMR spectrum (376.65 MHz, 296 K, chloroform-*d*, $\tau_m = 400$ ms) pertinent to an equilibrium mixture of **1a** and **2a**.

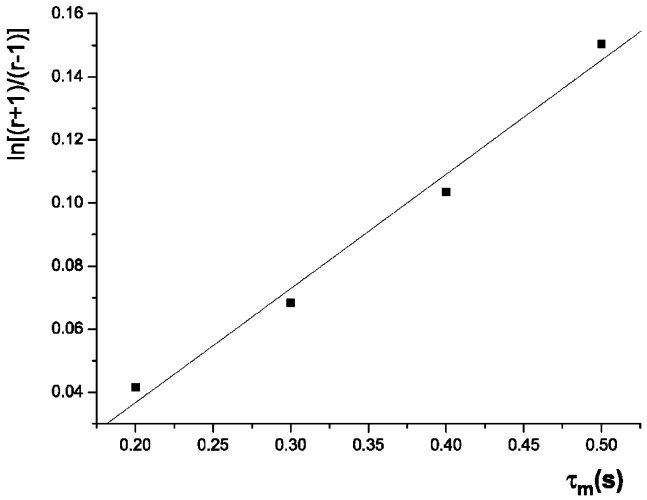

Figure 6. Plot of $\ln[(r+1)/(r-1)]$ vs τ_m for a solution of **1a** and **2a** obtained from ^{19}F-NOESY NMR spectra (376.65 MHz, 296 K, chloroform-*d*) recorded with different mixing times.

appreciably higher T_1 values (0.8 and 0.9 s for **2a** and **1a**, respectively) compared with those of the $OCH_{in}O$ resonances (0.4 and 0.7 s), which allows measurements in the linear part to be carried out with longer mixing times and, consequently, helps detect exchange NOEs of higher intensities. k_{obs} and the derived rate constants for the dissociative (k_{diss}) and associative (k_{ass}) processes are reported in Table 4.

The rate constant of the exchange process between external and encapsulated anions is comparable to that between the free and tetracoordinated cavitand ligands (entries 3/4 and 5/6). Interestingly, the rate constant values are very close to those previously reported for the reversible dimerization and encapsulated-benzene exchange of tetra urea calix[4]arenes.[8c] Both exchange processes are more than 1 order of magnitude accelerated passing from a relatively low polar solvent such as chloroform-*d* (relative permittivity, $\epsilon_r^{293K} = 4.81$) to a polar one, namely, nitromethane-d_3 ($\epsilon_r^{298K} = 35.94$) (compare entries

(25) (a) Shivanyuk, A.; Rissanen, K.; Kolehmainen, E. *Chem. Commun.* **2000**, 1107−1108. (b) Mansikkamäki, H.; Nissinen, M.; Rissanen, K. *Chem. Commun.* **2002**, 1902−1903.
(26) Pinalli, R.; Cristini, V.; Sottili, V.; Geremia, S.; Campagnolo, M.; Caneschi, A.; Dalcanale, E. *J. Am. Chem. Soc.* **2004**, *126*, 6516−6517.

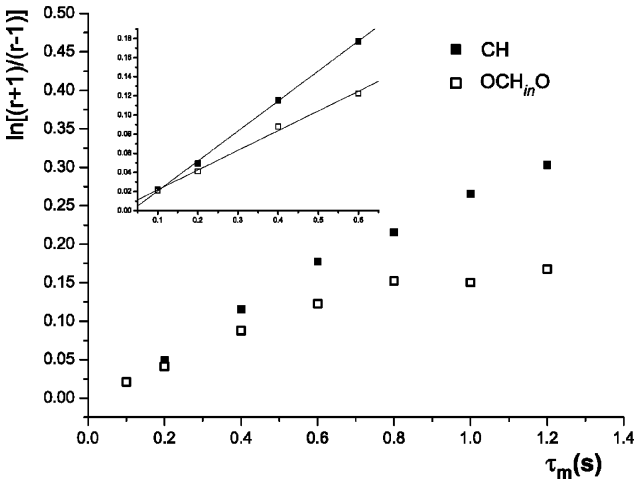

Figure 7. Plot of $\ln[(r + 1)/(r - 1)]$ vs τ_m for a solution of **1a** and **2a** obtained from ^{1}H-NOESY NMR spectra (400.13 MHz, 296 K, chloroform-*d*) recorded with different mixing times.

3−5 and 4−6). The free/coordinated exchange of tetracoordinated cavitand ligand probably occurs through a dissociative polar transition state, stabilized by a polar solvent. Once the cage **1a** is dissociated, $CF_3SO_3^-{}_{in}$ is no longer distinguishable from $CF_3SO_3^-{}_{out}$ because they undergo a very fast exchange. Only the closure of the cage causes the differentiation between $CF_3SO_3^-{}_{in}$ and $CF_3SO_3^-{}_{out}$. This explains why the two processes have the same rate constants. In agreement with such a consideration, the opening and closure processes of the coordinative cage studied in the absence of free cavitand afforded the same rate constant values (entry 2). The exchange process is remarkably slowed when coordination cage **1b** is considered, in which palladium is replaced by platinum. No exchange cross-peaks were observed in both ^{1}H- and ^{19}F-NOESY NMR spectra, even in nitromethane-d_3. This is in agreement with the strength of the M−N bond, which is known to be much higher for Pt than for Pd.

Conclusions

The combined use of PGSE, NOE, and EXSY NMR techniques has helped determine interionic structure, kinetic stability, and degree of anion encapsulation of coordination cages **1** in solution. Both interionic structure and kinetic stability are solvent dependent, while anion encapsulation is not.

In chloroform all counterions are positioned around the cationic cage and translate with it in solution. Interestingly, the anions are located not only in the four equatorial sites close to the metal centers, as expected, but also in the two polar pockets formed by the alkyl chains, suggesting a stabilizing role exerted by CH···X$^-$ interactions. The addition of a more polar solvent like nitromethane disrupts the ionic integrity of the cages, leaving only the internal triflate and an average of one or two anions connected to the cationic cage.

Anion inclusion is quantitative in solution as in the solid state, irrespective of the solvent. Since the encapsulation event is coincident with the cage self-assembly, the preference of the cavity for anion inclusion is complete, regardless of any stabilization offered to the anion by solvation.

The kinetic stability of these cages can be tuned by changing the coordinating metal and the solvent. The coarse tuning was obtained by forming the kinetically more inert Pt square-planar complexes instead of Pd ones. The corresponding cage **1b** is kinetically stable both in $CDCl_3$ and in CD_3NO_2 for a few seconds, the time frame limit of EXSY measurements. The fine-tuning can be controlled by choosing the solvent or the solvent mixture: reducing the solvent polarity led to a sizable increase of the k_{obs}. In this way the uptake and release of potential guests in solution can be precisely characterized.

A unique feature of this study has been the possibility to record independent sets of measurements by performing the experiments with two different nuclei, namely, ^{1}H and ^{19}F. The resulting cross validation of the data has given a highly reliable, comprehensive picture of the dynamic behavior of this class of coordination cages in solution. Since several other supramolecular assemblies present the ability to encapsulate anions or cations bearing heteroatoms,[27] this methodology can be of general use to assess the dynamic behavior of large aggregates in solution.

Experimental Section

General Procedures. All NMR measurements were performed on a Bruker Avance DRX 400 spectrometer operating at 400.13 MHz (^{1}H), 376.65 MHz (^{19}F), and 161.98 MHz (^{31}P), equipped with a GREAT 1/10 gradient unit and a QNP probe with a Z-gradient coil. Cavitands **2a**,**b** and metal complexes **3a**,**b** were prepared according to published procedures.[19]

Preparation of the Coordination Cages. To a solution of cavitand **2a** (0.003 mmol, in 0.5 mL of chloroform-*d*) was added complex **3a** (0.006 mmol). Cage **1a** immediately formed. The solvent was then removed under vacuum, and the solid cage **1a** was dissolved respectively in 0.5 mL of CD_2Cl_2, benzene-d_6, and nitromethane-d_3/chloroform-*d* (7/1). Cage **1b** was prepared in the same way starting from cavitand **2b** and metal precursor **3b** and then dissolved in $CDCl_3$ and CD_3NO_2. For the PGSE experiments concentrations see the caption to Table 2.

Spectroscopic Resonances Attribution of Cavitand 2a and Cage 1a. 2a: ^{1}H NMR (300 MHz, $CDCl_3$) δ 0.88 (t, 12H, CH_3), 1.26−1.40 [m, 72H, $CH_2(CH_2)_9CH_3$], 2.19 [m, 8H, $CHCH_2(CH_2)_9CH_3$], 4.59 (d,

Table 4. Rate Constants k_{obs}, k_{diss}, and k_{ass} Determined at 296 K for Cage **1a** and Cavitand **2a** in Chloroform-*d* and Nitromethane-d_3 at Different Molar Fractions (X)

entry	cage/cavitand	observed nucleus	solvent	$X_{CF_3SO_3^-{}_{in}}$	$X_{CF_3SO_3^-{}_{out}}$	$X_{\mathbf{2a}}$	$X_{\mathbf{1a}}$	k_{obs}(s^{-1})	k_{diss}(s^{-1})	k_{ass}(s^{-1})
1	**1a**	^{1}H	$CDCl_3$			1.00	0.00			
2	**1a**	^{19}F	$CDCl_3$	0.90	0.10			0.32 ± 0.08	0.29 ± 0.08	0.03 ± 0.08
3	**1a**/**2a**	^{1}H	$CDCl_3$			0.33	0.67	0.30 ± 0.04	0.20 ± 0.04	0.10 ± 0.04
4	**1a**/**2a**	^{19}F	$CDCl_3$	0.10	0.90			0.33 ± 0.06	0.30 ± 0.06	0.03 ± 0.06
5	**1a**/**2a**	^{1}H	CD_3NO_2			0.12	0.88	5.2 ± 0.8	4.6 ± 0.8	0.6 ± 0.8
6	**1a**/**2a**	^{19}F	CD_3NO_2	0.03	0.97			5.0 ± 0.8	4.8 ± 0.8	0.2 ± 0.8
7	**1b**	^{19}F	$CDCl_3$	0.90	0.10			*a*	*a*	*a*
8	**1b**	^{19}F	CD_3NO_2	0.90	0.10			*a*	*a*	*a*

[a] No exchange cross-peaks were observed.

4H, OCH_{in}O, J = 6.7 Hz), 4.79 [t, 4H, $CHCH_2(CH_2)_9CH_3$], 6.08 (d, 4H, OCH_{out}O, J = 6.7 Hz), 7.25 (s, 4H, ArH).

1a: ^{1}H NMR ($CDCl_3$, 300 MHz) δ 0.81 (t, 24H, CH_3, J = 6.8 Hz), 1.20−1.34 [m, 128H, $CH_3(CH_2)_8$], 1.48 [bs, 16H, $CHCH_2CH_2(CH_2)_8CH_3$], 2.43 [m, 16H, $CHCH_2(CH_2)_9CH_3$] partially superimposed to 2.55 (bs, 8H, $Ph_2PCH_2CH_2CH_2PPh_2$), 2.95 (bs, 16H, $Ph_2PCH_2CH_2CH_2PPh_2$), 4.03 (d, 8H, OCH_{in}O, J = 7.3 Hz), 4.38 (t, 8H, CH, J = 8.2 Hz), 6.07 (d, 8H, OCH_{out}O, J = 7.3 Hz), 7.21−7.60 (m, 80H, C_6H_5), 7.94 (s, 8H, ArH); ^{31}P NMR ($CDCl_3$, 81 MHz) δ 10.1 (s); ^{19}F NMR ($CDCl_3$, 188.3 MHz) δ −78.2 ($CF_3SO_3^-{}_{out}$), −81.5 ($CF_3SO_3^-{}_{in}$).

***T*$_1$ Measurements.** A solution of cavitand **2a** and the cage **1a** in chloroform-*d* was degassed by three freeze−pump−thaw cycles on a vacuum line. Measurements were performed at 298 K using the standard inversion recovery pulse sequence with a d_1 delay time of 10 s. The semilogarithmic trend of the ^{1}H and ^{19}F peak intensities as a function of the evolution time was fitted using the XWinNMR Bruker software. Important T_1 values are 0.8 and 0.9 s for CH resonances of **2a** and **1a**, respectively; 0.4 and 0.7 s for OCH_{in}O resonance of **2a** and **1a**, respectively; and 0.7 s for both $CF_3SO_3^-{}_{in}$ and $CF_3SO_3^-{}_{out}$.

PGSE Measurements. All the PGSE NMR measurements were performed by using the standard stimulated echo pulse sequence[28] at 296 K without spinning. The shape of the gradients was rectangular, their duration (δ) was 4−5 ms, and their strength (G) was varied during the experiments. All the spectra were acquired using 32K points and a spectral width of 5000 (^{1}H) and 18 000 (^{19}F) Hz and processed with a line broadening of 1.0 (^{1}H) and 1.5 (^{19}F) Hz. The experiments were carried out with a total recycle time of 5 s. The semilogarithmic plots of $\ln(I/I_0)$ versus G^2 were fitted using a standard linear regression algorithm obtaining an R factor always better than 0.99. Different values of Δ, "nt" (number of transients), and number of different gradient strengths (G) were used for different samples. For example, for the measurements of coordination cages and cavitands in chloroform-*d*, the "nt" values were 48 (^{1}H) and 96 (^{19}F). OCH_{in}O, OCH_{out}O, CH, $CF_3SO_3^-{}_{in}$, and $CF_3SO_3^-{}_{out}$ resonances were usually investigated.

The dependence of the resonance intensity (I) on a constant waiting time and on a varied gradient strength (G) is described by eq 1:

$$\ln\frac{I}{I_0} = -(\gamma\delta)^2 D_t\left(\Delta - \frac{\delta}{3}\right)G^2 \qquad (1)$$

where I = intensity of the observed spin−echo, I_0 = intensity of the spin−echo without gradients, D = diffusion coefficient, Δ = delay between the midpoints of the gradients, δ = length of the gradient pulse, and γ = magnetogyric ratio. The diffusion coefficient D_t is directly proportional to the slope of the regression line ($-m$) divided by $\Delta - \delta/3$, and its value was estimated by measuring the $-m/(\Delta - \delta/3)$ parameter for a sample of HDO (5%) in D_2O (known diffusion coefficient: 1.902×10^{-9} m^2/s)[29] under the same conditions as those for compounds.

According to the Stokes−Einstein eq 2, D_t is proportional to $1/r_H$ (where r_H represents the hydrodynamic radius of the diffusing particle).

$$D_t = \frac{kT}{c\pi\eta r_H} \qquad (2)$$

where k is the Boltzmann constant, T is the absolute temperature, c is a numerical factor that depends on the size and shape of the solute and the hydrodynamic behavior of the solute−solvent system,[28] and η is the viscosity of the pure solvent. By applying eq 2 to samples of **1a** and **2a** containing tetrakis(trimethylsilyl)silane (TMSS) as internal standard, the average hydrodynamic radii for the anionic and cationic moieties were estimated.[30]

The measurement uncertainty was estimated by determining the standard deviation of m by performing experiments with different Δ values. Standard propagation of errors analysis yielded a standard deviation of approximately 3% in the hydrodynamic radius r_H.

HOESY Measurements. Two-dimensional ^{19}F,^{1}H-HOESY NMR experiments were acquired using the standard four-pulse sequence or the modified version.[31] The number of transients was 64K and the number of data points was 512. Quantitative spectra were acquired using a 7 s relaxation delay and 300 ms mixing times. The evaluation of the NOE intensities was carried out taking into account that their volumes are proportional to

$$\frac{n_I n_S}{n_I + n_S}$$

where n_I and n_S are the number of equivalent I and S nuclei, respectively.[23]

EXSY Measurements. ^{1}H-NOESY and ^{19}F-NOESY[32] NMR experiments were acquired at 296 K by the standard three-pulse sequence or by the PFG version.[33] The number of transients and the number of data points were chosen according to the sample concentration and the desired final digital resolution. For example, for the ^{1}H-NOESY NMR measurements of a solution of **1a** and **2a** in chloroform-*d*, the number of transients was 64K and the number of data points was 256, and the "nt" values were 48. Quantitative ^{1}H-NOESY and ^{19}F-NOESY NMR experiments were carried out with a relaxation delay of 5 s and a mixing time ranging from 0.1 to 1.2 s. The auto- and cross-peak volumes were determined using XWinNMR Bruker software after phase and baseline corrections in both dimensions. The volume uncertainty was estimated by determining the volume of noise signal in a "blank space" of the spectrum.

The use of 2D-NOESY for chemical kinetics was first proposed by Jeener and Ernst[32] and was called 2D-EXSY (exchange spectroscopy).[20] 2D-EXSY spectra arise from noncoherent magnetization transfer that can take place by exchange of nuclei between nonequivalent sites and avoids the cross-relaxation between sites with different resonance frequency. 2D-EXSY[20] can measure a rate constant k on the order of 10^{-1}−10^2 s^{-1}. The upper limit is governed by the difference in chemical shift ($k \ll \omega_a - \omega_b$), and the lower limit is dictated by the relaxation time T_1 ($k \approx 1/T_1$). For an uncoupled system of spins A and B, with the simplification of equal spin−lattice relaxation time, the rate constant k_{obs} is related to the mixing time τ_m by eq 3:

$$\ln\left(\frac{r+1}{r-1}\right) = k_{obs}\tau_m \qquad (3)$$

In eq 3 the term r is related to the volumes of the cross and diagonal signal (I) and to the molar fraction of the species A and B (X) by eq 4:

$$r = \frac{4X_aX_b(I_{aa} + I_{bb})}{(I_{ab} + I_{ba})} - (X_a - X_b) \qquad (4)$$

Since the system is in equilibrium (A ⇔ B), it is possible to determinate the direct k_{a-b} and the reverse k_{b-a} rate constant by eqs 5 and 6:

(27) (a) Johnson, D. W.; Raymond, K. N. *Supramol. Chem.* **2001**, *13*, 639−659. (b) Mann, S.; Huttner, G.; Zsolnai, L.; Heinze, K. *Angew. Chem., Int. Ed. Engl.* **1996**, *35*, 2808−2809. (c) McMorran, D. A.; Steel, P. J. *Angew. Chem., Int. Ed.* **1998**, *37*, 3295−3297. (d) Fiedler, D.; Pagliero, D.; Brumaghim, J. L.; Bergam, R. G.; Raymond, K. N. *Inorg. Chem.* **2004**, *43*, 846−848.

(28) Valentini, M.; Rüegger, H.; Pregosin, P. S. *Helv. Chim. Acta* **2001**, *84*, 2833−2853, and references therein.

(29) Tyrrell, H. J. W.; Harris, K. R. *Diffusion in Liquids*; Butter-Worth: London, 1984.

(30) Zuccaccia, D.; Sabatini, S.; Bellachioma, G.; Cardaci, G.; Clot, E.; Macchioni, A. *Inorg. Chem.* **2003**, *42*, 5465−5467.

(31) Lix, B.; Sönnichsen, F. D.; Sykes, B. D. *J. Magn. Reson. A* **1996**, *121*, 83−87.

(32) Jeener, J.; Meier, B. H.; Bachmann, P.; Ernst, R. R. *J. Chem. Phys.* **1979**, *71*, 4546−4553.

(33) Wagner, R.; Berger, S. *J. Magn. Reson. A* **1996**, *123*, 119−121.

$$k_{a-b} = X_b k_{obs} \quad (5)$$

$$k_{b-a} = X_a k_{obs} \quad (6)$$

In our case in the ^{1}H-NOESY experiment A and B represent cage **1a** and cavitand **2a**, while in the ^{19}F-NOESY A and B represent the $CF_3SO_3^-{}_{in}$ and $CF_3SO_3^-{}_{out}$ anion, so the direct k_{a-b} rate constant describes the dissociation of cage **1a** and the consequent exit of the internal anion (k_{diss}). On the other hand, the reverse k_{b-a} rate constant describes the cage self-assembly and the inclusion of one external anion in the cage (k_{ass}).

The rate constant k_{obs} could be obtained (1) as the slope of a linear plot of an appropriate experimental quantity versus τ_m if the mixing time were variable (see eq 3) or (2) if only one mixing time is available by applying directly eq 3.

The linear regression of experimental values within their errors (estimated by standard propagation of errors analysis from the errors of the peak volume) was performed by using the software package Microcal Origin 7.0, which obtains the slope of regression and its standard deviation.

Acknowledgment. This work was supported by MURST through FIRB-Nanoorganization of Materials with Magnetic and Optical Properties, COFIN 2003-Proprietà di singole molecole ed architetture molecolari funzionali supportate, and COFIN 2004-Nuove strategie per il controllo delle reazioni: interazione di frammenti molecolari con siti metallici in specie non convenzionali.

JA042265+